Effective Theories in Hadron and Nuclear Physics

Coulomb and finite-range effects in femtoscopic correlations

Controlled matching and the $\alpha\alpha$ benchmark

Amador García Lorenzo

With M. Albaladejo and J. Nieves; $\alpha\alpha$ with A. Feijoo

Instituto de Física Corpuscular, CSIC–Universitat de València

The on-shell amplitude does not fix a finite-source correlation

Construction: Gell-Mann–Goldberger two-potential decomposition

$$H = H_C + V_S, \qquad H_C = H_0 + V_C, \qquad T = T_C + T_{SC}$$

A common contact resummation fixes the on-shell amplitude and its Coulomb-distorted exterior wave.

Observable: finite-source sensitivity

The correlation folds the scattering probability with a source of radius R. For R comparable to the strong range R_S, it retains a source-weighted interior contribution beyond the exterior-wave construction.

Effective-range information constrains the integrated norm; the source profile controls the residual correction.

Validity: independent expansions

$$pR_S \quad \text{and} \quad \frac{R_S}{R}$$

ERE truncation and source variation are controlled separately, while $\eta = Z_1 Z_2 \alpha\mu/p$ is not expanded and Coulomb is resummed.

Result: benchmark and application. Square-well, Reid soft-core and ALICE pp benchmarks precede $\alpha\alpha$ with fixed elastic input and independent source, composition and resolution parameters.

Femtoscopy averages the full scattering wave over a finite source

Observable: Koonin–Pratt kernel

$$C(p) = \int d^3\boldsymbol{r}\, \widetilde{S}(r) \left|\Phi_{\boldsymbol{p}}^{(-)}(\boldsymbol{r})\right|^2 = \int_0^\infty dr\, S(r)\, \mathcal{A}(p,r),$$

$$\mathcal{A}(p,r) = \frac{1}{2}\int_{-1}^{1} d\cos\theta \left|\Phi_{\boldsymbol{p}}^{(-)}(\boldsymbol{r})\right|^2 .$$

Input: spherical Gaussian source

$$\widetilde{S}(r) = \frac{e^{-r^2/(4R^2)}}{(4\pi R^2)^{3/2}},$$

$$S(r) = 4\pi r^2 \widetilde{S}(r),$$

$$\sqrt{\langle r^2\rangle} = \sqrt{6}\, R, \qquad \int_0^\infty dr\, S(r) = 1.$$

Construction: retained dynamics

Nonrelativistic elastic kernel, $E_p = p^2/(2\mu)$: nuclear pp is truncated to ${}^1S_0$, while Coulomb retains all partial waves.

Chaoticity, smoothness and equal time make the source local and diagonal.

Validity: source expansion over R_S

$$\frac{\widetilde{S}(r)}{\widetilde{S}(0)} = 1 - \frac{r^2}{4R^2} + \mathcal{O}\left(\frac{r^4}{R^4}\right), \qquad \epsilon_S \equiv \frac{R_S^2}{4R^2} \ll 1$$

Coulomb must be resummed when $p \sim k_C$

Construction: exact Coulomb scattering state

$\psi_{\boldsymbol{p}}^{(+)}(\boldsymbol{r}) = e^{-\pi\eta/2}\Gamma(1+i\eta)M(-i\eta,1;ipr-i\boldsymbol{p}\cdot\boldsymbol{r})\, e^{i\boldsymbol{p}\cdot\boldsymbol{r}}$

Input: Coulomb threshold scale

$$V_C(r) = \frac{Z_1 Z_2 \alpha}{r}, \qquad \eta = \lambda\frac{k_C}{p},$$

$$k_C = |Z_1 Z_2|\alpha\mu, \qquad \lambda = \mathrm{sign}(Z_1 Z_2),$$

$$k_C \simeq 3.4 \text{ MeV } (pp), \quad k_C \simeq 54.4 \text{ MeV } (\alpha\alpha).$$

Coulomb ladders contribute at all orders for $p \lesssim k_C$.

Construction: normalization and phases

$$C_\eta^2 = \left|\psi_{\boldsymbol{p}}^{(\pm)}(\boldsymbol{0})\right|^2 = \frac{2\pi\eta}{e^{2\pi\eta}-1},$$

$$e^{2i\sigma_\ell} = \frac{\Gamma(\ell+1+i\eta)}{\Gamma(\ell+1-i\eta)}.$$

Short-range matrix elements are evaluated between Coulomb-distorted states.

Observable: finite-source Coulomb contribution

$$C_C(p) = \int d^3\boldsymbol{r}\, \widetilde{S}(r)|\psi_{\boldsymbol{p}}^{(+)}(\boldsymbol{r})|^2, \qquad C_C(p) \xrightarrow{R\to 0} C_\eta^2.$$

Coulomb subtraction preserves ERE and unitarity

Construction: contact resummation in the Coulomb basis

$$T_{SC}(p) = \frac{C_\eta^2 e^{2i\sigma_0}}{C_0^{-1}(p^2) - J_0(E_p)} = -\frac{2\pi}{\mu} C_\eta^2 e^{2i\sigma_0} f_{SC}(p),$$

$$J_0(E_p) = \langle \mathbf{0} | G_C^{(+)}(E_p) | \mathbf{0} \rangle, \qquad T = T_C + T_{SC}.$$

Input: renormalized Coulomb-modified ERE

$$\mathcal{K}_0(p) = -\frac{2\pi}{\mu}\left[C_0^{-1}(p^2) - J_0(0)\right]$$
$$= -\frac{1}{a_0} + \frac{1}{2} r_0 p^2 + v_2 p^4 + \cdots ,$$

$$f_{SC}^{-1}(p) = \mathcal{K}_0(p) - 2p\eta H^\lambda(\eta).$$

$J_0(0)$ is absorbed into the short-range input; a_0, r_0, v_2 are Coulomb-modified coefficients.

Construction: known Coulomb cut

$$H^\lambda(\eta) = h^\lambda(\eta) + i\frac{C_\eta^2}{2\eta}$$

Validity: elastic unitarity

$$f_{SC}^{-1} = C_\eta^2 p(\cot\delta_0 - i),$$
$$\mathrm{Im}\, f_{SC}^{-1} = -pC_\eta^2.$$

Total phase: $\sigma_0 + \delta_0$.

The amplitude fixes the exterior wave, not the interior

Construction: Coulomb-distorted exterior wave

$$\left[\Phi_{\boldsymbol{p}}^{(-),\mathrm{asy}}(\boldsymbol{r})\right]^{*} = \psi_{-\boldsymbol{p}}^{(+)}(\boldsymbol{r}) + \frac{T_{SC}(p)\, G_C^{(+)}(E_p; r)}{e^{-\pi\eta/2}\Gamma(1+i\eta)}$$

Input: coordinate-space Coulomb propagator

$$G_C^{(+)}(E_p; r) = -\frac{\mu}{2\pi r}\Gamma(1+i\eta) W_{-i\eta,1/2}(-2ipr), \qquad r > 0$$

The Whittaker representation gives the radial response analytically; its normalization is fixed by T_{SC}.

Validity: finite-range matching

- Exact contact-model wave for $r > 0$.
- Exact exterior representation for $r > R_S$ when V_S has finite range.
- Continuation into $r < R_S$ leaves a finite-range remainder.

Observable: interior remainder

all Coulomb waves; nuclear $\ell = 0$

Exterior and interior terms separate in the correlation

Observable: exact decomposition in the retained nuclear S wave

$$C(p) = C_C(p) + \Delta C_{\mathrm{LL}}(p) + \delta C(p)$$

Input: exact Coulomb source integral

$$C_C = \int d^3\boldsymbol{r}\, \widetilde{S}(r) |\psi_{\boldsymbol{p}}^{(+)}(\boldsymbol{r})|^2$$

Exact spatial Coulomb wave, summed over all partial waves.

Construction: exterior-wave nuclear term

$$\Delta C_{\mathrm{LL}} = \int_0^\infty dr\, S(r) \left(|\phi_0^{\mathrm{asy}}|^2 - |\psi_0|^2 \right)$$

Fixed by on-shell f_{SC}, the source and the ERE truncation.

Result: finite-range remainder

$$\delta C = \int_0^{R_S} dr\, S(r) \left(|\phi_0^{\mathrm{exact}}|^2 - |\phi_0^{\mathrm{asy}}|^2 \right)$$

Source-weighted interior norm on $r < R_S$, not fixed by the on-shell amplitude at fixed momentum.

Here LL labels the exterior-wave term; the original framework also includes finite range.

The square well separates source and momentum dependence

Input: solvable singlet benchmark $V_S = -V_0\Theta(R_S - r)$, $V_0 = 12.46$ MeV, $R_S = 2.70$ fm, plus repulsive Coulomb.

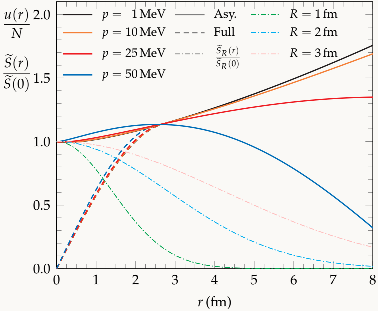

Observable: source weighting. For $R = 1$–3 fm, source variation overlaps the interior mismatch at $r < R_S$.

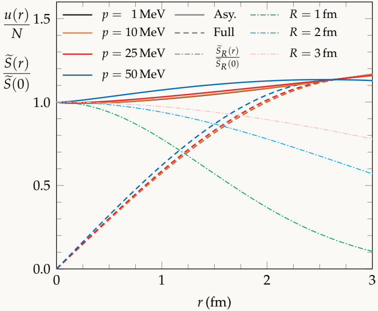

Result: weak momentum variation. For $p = 1$–50 MeV, the normalized interior mismatch changes only weakly with momentum.

ERE fixes the norm; source variation fixes the residual

Input: Wronskian norm identity for a local, energy-independent finite-range potential

$$\frac{d_0(p)}{2} \equiv \frac{\partial \mathcal{K}_0}{\partial p^2} = \frac{\int_0^{R_S} dr\, r^2 \left(|\phi_0^{\mathrm{asy}}|^2 - |\phi_0^{\mathrm{exact}}|^2\right)}{C_\eta^2 |f_{SC}(p)|^2}, \qquad d_0(p) = r_0 + 4v_2 p^2 + \cdots$$

Construction: exact source-dependent separation

$$\delta C(p) = -2\pi \widetilde{S}(0) d_0(p) C_\eta^2 |f_{SC}(p)|^2 + \delta C_{\mathrm{src}}(p),$$

$$\delta C_{\mathrm{src}}(p) = 4\pi \int_0^{R_S} dr\, r^2 [\widetilde{S}(r) - \widetilde{S}(0)] \times \left(|\phi_0^{\mathrm{exact}}|^2 - |\phi_0^{\mathrm{asy}}|^2\right).$$

Result: Gaussian approximation

$$\delta C(p) \simeq -\frac{d_0(p) C_\eta^2 |f_{SC}(p)|^2}{4\sqrt{\pi} R^3}$$

Validity: separate controls

Source: $\delta C_{\mathrm{src}} \simeq 0$ when $\widetilde{S}(r)$ varies slowly over the norm integral.

Threshold: $d_0(p) = r_0 + O(p^2)$.

The norm correction converges as the source radius grows

Input: controlled singlet diagnostic Same on-shell amplitude in all curves; identical-particle exchange omitted.

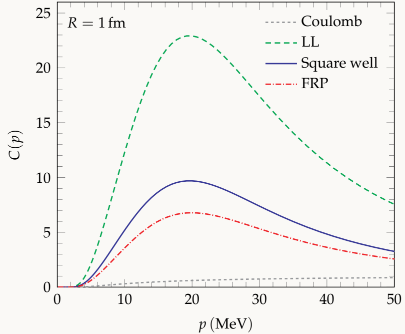

Observable: $R = 1$ fm. Peak $C_{\rm LL} \simeq 23$ versus $C_{\rm exact} \simeq 9.5$; source variation remains after FRP.

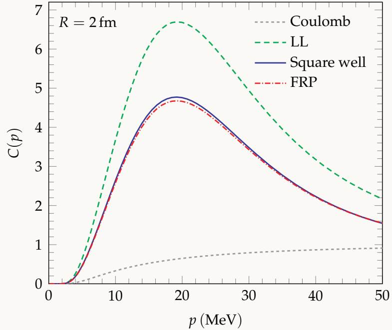

Result: $R = 2$ fm. Peak $C_{\rm LL} \simeq 6.7$ versus $C_{\rm exact} \simeq 4.7$; the r_0 correction nearly saturates the difference.

Fermi symmetry fixes the physical pp weights

Observable: unpolarized proton correlation

$$C_{pp} = \frac{1}{4}C_{[S]C} + \frac{3}{4}C_{[A]C} + \frac{1}{2}\Delta C_{\mathrm{LL}} + \frac{1}{2}\delta C$$

Construction: Coulomb exchange kernel

$$C_{[S,A]C} = \int d^3\boldsymbol{r}\,\widetilde{S}(r)\left|\frac{\psi(\boldsymbol{r},\boldsymbol{p}) \pm \psi(-\boldsymbol{r},\boldsymbol{p})}{\sqrt{2}}\right|^2$$

Singlet (1/4): symmetric spatial wave and even ℓ.

Triplet (3/4): antisymmetric spatial wave and odd ℓ.

The projectors retain the corresponding even and odd Coulomb partial waves.

Input: nuclear truncation

Only ${}^1S_0$ is retained in the nuclear contribution in the correlation-dominated momentum region.

Singlet averaging and spatial symmetrization give the common factor 1/2 in both strong terms.

Validity: noninteracting limit

$$C_{pp}(p)\big|_{V_S=V_C=0} = 1 - \frac{1}{2}e^{-4p^2R^2}$$

Finite-range completion removes most of the Reid pp excess

Input: Reid soft-core amplitude $a_0 = -7.78$ fm, $r_0 = 2.72$ fm, $v_2 = -0.028\, r_0^3$.

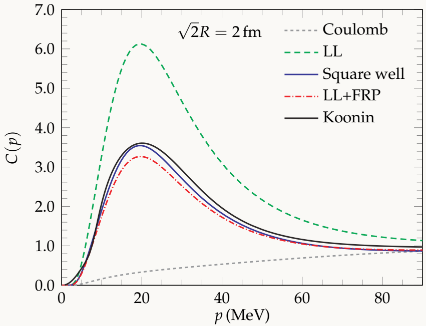

Result: $\sqrt{2}R = 2$ fm. Peak $\simeq 6.2$ (LL) $\to 3.3$ (FRP), compared with $\simeq 3.6$ in Koonin's calculation.

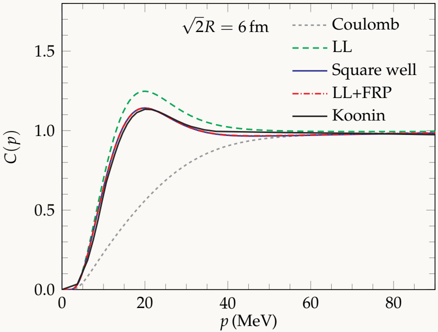

Result: $\sqrt{2}R = 6$ fm. Peak $\simeq 1.23$ (LL) $\to 1.14$ (FRP), in agreement with Koonin.

Source variation dominates the compact-source correction

Construction: finite-source parametrization

$$\delta C \simeq -\beta \frac{d_0(p) C_\eta^2 |f_{SC}(p)|^2}{4\sqrt{\pi} R^3}.$$

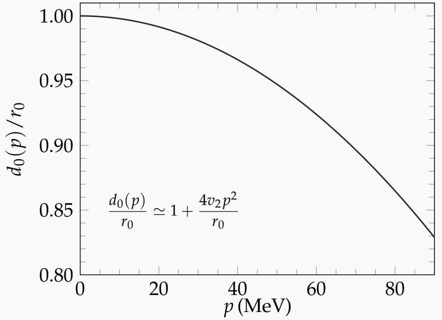

Observable: ERE momentum dependence. $d_0/r_0 \simeq 0.99$ near the peak; corrections increase only for $p \gtrsim 40$–50 MeV.

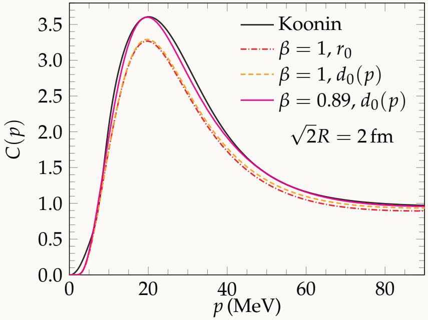

Result: source-profile response. $\beta = 0.89$ is calibrated to the compact-source peak; no universal β is assumed.

Finite-range completion improves ALICE pp without a refit

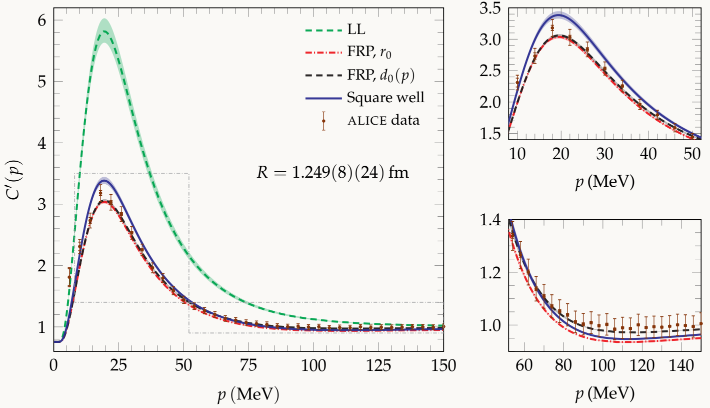

Result: FRP suppresses the peak excess; momentum-dependent $d_0(p)$ improves the tail.

Construction: pair composition

$$C' = 1 + \lambda_{pp}(C_{pp} - 1) + \lambda_{pp_\Lambda}(C_{pp_\Lambda} - 1)$$

$p\Lambda$ feed-down is mapped to the reconstructed pp momentum.

Input: fixed externally

$R = 1.249(8)(24)$ fm,

$\lambda_{pp} = 0.67$,

$\lambda_{pp_\Lambda} = 0.203$,

$\beta = 1$.

Validity: bands propagate source-radius uncertainty. No input is refitted to these pp data.

Resonant $\alpha\alpha$ adds a D wave at fixed scattering input

Construction: change of physical channel

	pp	$\alpha\alpha$
Coulomb strength	$Z_1 Z_2 = 1$	$Z_1 Z_2 = 4$
Statistics	spin-$\frac{1}{2}$ fermions	spin-zero bosons
Strong waves	singlet S wave	resonant $S + D$ waves
Scattering input	CF benchmark	fixed before CF fits

Input: common nuclear construction

Both systems use amplitudes distorted by Coulomb and a finite-range term.

The near-threshold ^{8}Be 0^+ pole and broad 2^+ resonance probe separated momenta.

Observable: data-set response

For each data set, R, σ_p and the pair fractions are determined independently.

Validity: partial-wave matching

For $\ell > 0$, exterior and short-distance terms require one common matching prescription.

Transfer logic: the elastic amplitude is fixed before the correlation fit

VALIDATED IN pp
Square well, Reid and ALICE

$\Longrightarrow$

FIXED IN $\alpha\alpha$
Coulomb-distorted $S + D$ input

$\Longrightarrow$

TESTED IN DATA
Pochodzalla and Ghetti

The ^{8}Be poles define separated momentum scales

$p_{0^+} \simeq 18.5$ MeV and $p_{2^+} \simeq 108$ MeV define distinct momentum scales.

FIXED: Coulomb conventions

$$Z_\alpha = 2,\ \mu = M_\alpha/2,\ E = p^2/(2\mu).$$

$$k_C = 4\alpha_{\rm em}\mu \simeq 54.4\ \text{MeV},\ \eta(p_{0^+}) \simeq 2.9.$$

Nonperturbative Coulomb at the near-threshold pole.

FIXED: corrected-ERE pole

$$E_\star = \frac{p_\star^2}{2\mu} = E_R - \frac{i}{2}\Gamma_R,$$

$$|a_0| \sim 10^3\ \text{fm},\ r_0 \simeq 1.1\ \text{fm}.$$

$|a_0| \gg r_0$ and $\Gamma_{0^+} \ll E_{0^+}$.

INFERRED FROM THE POLES: separated momentum scales

Channel	Energy above threshold	Width	Relative momentum
0^+	$\simeq 92$ keV	$\simeq 5$–6 eV	$p \simeq 18.5$ MeV
2^+	3.122 MeV	1.513 MeV	$p \simeq 108$ MeV

Limit: the 0^+ values use the corrected ERE input, not an average over the three descriptions.

Fixed S-wave inputs agree near threshold and diverge above it

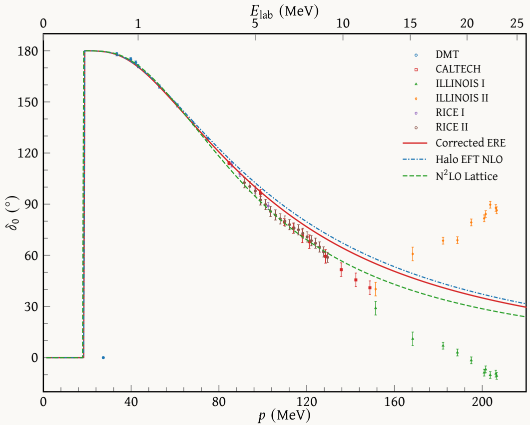

FIXED: Coulomb-modified ERE

$$K_0(p) = -\frac{1}{a_0} + \frac{r_0}{2}p^2 + v_2 p^4 + \cdots$$

Corrected ERE; halo EFT NLO; lattice N^{2}LO.

RESULT

Corrected ERE and halo EFT overlap near the 0^+ pole. The lattice curve departs at larger momentum.

LIMIT OF THE COMPARISON

Central phase-shift inputs are shown. Their scattering coefficients remain fixed throughout the CF fits.

Phase shifts fix one D-wave description of the 2^+ resonance

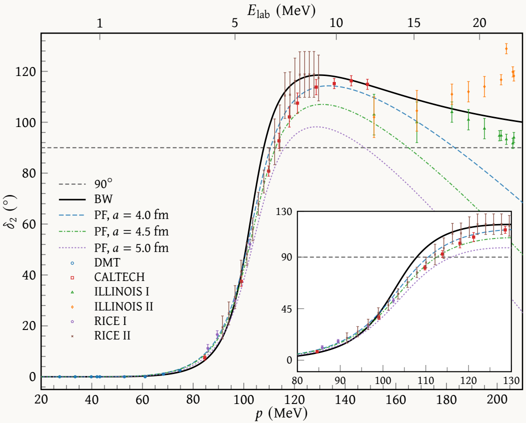

MODEL: one-level Coulomb R-matrix

$$\tan(\delta_2 + \omega_2) = \frac{\Gamma_2(E)}{2(E_R - E)}$$

$$\Gamma_2(E) = \Gamma_R \frac{P_2(E, a_c)}{P_2(E_R, a_c)}$$

$P_2 = \rho/|H_2^+(\eta,\rho)|^2$, $\omega_2 = \arg H_2^+$,
$\rho = p a_c$.

FIXED FROM PHASE SHIFTS

$E_R = 3.122$ MeV, $\Gamma_R = 1.513$ MeV, and $a_c = 4.5$ fm.

RESULT / LIMIT

The adopted curve uses $a_c = 4.5$ fm. This same D-wave amplitude enters all three CF fits.

The $\alpha\alpha$ kernel requires a matched short-distance completion

FIXED SYMMETRY

$\Psi^{(E)}(\boldsymbol{r}) = \dfrac{\Psi(\boldsymbol{r}) + \Psi(-\boldsymbol{r})}{\sqrt{2}}$; odd waves vanish for spin-zero bosons.

FITTED SOURCE SCALE

$S_R(r) = \dfrac{e^{-r^2/(4R^2)}}{(4\pi R^2)^{3/2}}$; R is determined separately for each data set.

INFERRED CORRELATION: exterior response plus interior completion

$$C_{\alpha\alpha}(p;R) = C_C^{(E)}(p;R) + \Delta C_{\mathrm{FRP}}^{(E)}(p;R)$$

$$+\,8\pi \sum_{\ell=0,2,\ldots} (2\ell+1) \int_0^\infty dr\, r^2 S_R(r)\left(|\Psi_\ell|^2 - |\Phi_\ell|^2\right),$$

$\Phi_\ell = \Psi_\ell|_{V_S=0}$; the retained strong waves are $\ell = 0, 2$.

FIXED: explicit S-wave completion

$$\Delta C_{\mathrm{FRP},0}^{(E)} \simeq -4\pi d_0(p) C_\eta^2 |f_0(p)|^2 S_R(0)$$

$$d_0(p) = 2\frac{\partial K_0}{\partial p^2} = r_0 + 4v_2 p^2 + \cdots$$

LIMIT: short-distance matching

$S_R(r) \simeq S_R(0)$ only over the strong-interaction region. For $\ell > 0$, the singular exterior continuation and interior remainder require one common prescription.

Source and finite-range strength are fitted at fixed amplitudes

FIT MODEL

$$C_{\mathrm{raw}}(p;R) = N\left[1 + \lambda\left(C_{\mathrm{ext}}(p;R) - 1\right) + \beta C_{\mathrm{FRP}}(p;R) + \gamma C_{^9\mathrm{Be}}(p)\right]$$

C_{ext} contains Coulomb, exchange and exterior strong waves; C_{FRP} is the nominal S-wave completion.

FIXED

S- and D-wave scattering amplitudes.

Coulomb-modified ERE coefficients.

Exterior kernel and nominal S-wave FRP shape.

FITTED

Source: R and long-distance dilution λ.

Interior strength: β, with $\beta = 0$ exterior-only and $\beta = 1$ nominal completion.

Composition and response: γ, N, σ_p.

INFERRED / LIMITED

R and β are compared across fixed nuclear inputs.

λ and β are independent fit directions.

Pochodzalla retains a constrained residual background; Ghetti is compatible with zero.

Sequential ^{9}Be feed-down has a fixed endpoint

FIXED LEVEL

$^9\mathrm{Be}(5/2^-)$

$$E_x = 2.4294(13)\ \mathrm{MeV},$$
$$\Gamma_9 = 0.78(13)\ \mathrm{keV}$$

→

ADOPTED CHANNEL

$$n + (\alpha\alpha)_{\ell=2}$$
$$Q_9 = 0.856\ \mathrm{MeV} < E_R[^8\mathrm{Be}(2^+)]$$

The continuum samples the low-energy 2^+ tail.

→

FIXED ENDPOINT

$$x = p/p_{\max}$$
$$p_{\max} = \sqrt{2\mu Q_9} = 56.5\ \mathrm{MeV}$$

ADOPTED THRESHOLD LAW

$$k^2 = 2\mu_{n,(\alpha\alpha)} Q_9 (1 - x^2)$$
$$d\Phi_3 \propto p^2 k\, dp, \qquad \mathcal{M}_{21} \propto p^2 k\, g_{21}$$
$$g_{21} \simeq \mathrm{const.} \implies \frac{dN}{dp} \propto p^6 k^3$$
$$C_{9\mathrm{Be}}(p) = C_0 x^6 (1 - x^2)^{3/2} \theta(1 - x)$$

FITTED RESPONSE

$$C_{\mathrm{fit}}(p) = \frac{1}{\mathcal{N}_\sigma(p)} \int_0^\infty dq\, e^{-(q-p)^2/(2\sigma_p^2)} C_{\mathrm{raw}}(q)$$
$$\mathcal{N}_\sigma(p) = \int_0^\infty dq\, e^{-(q-p)^2/(2\sigma_p^2)}$$

σ_p is fitted; the normalization keeps the Gaussian response on the physical half-line $q \geq 0$.

LIMIT: $g_{21} \simeq$ const. supplies the leading centrifugal template; explicit penetrabilities and the 2^+ line shape are omitted, while γ remains a free normalization.

[1] D. R. Tilley et al., Nucl. Phys. A **745**, 155 (2004), Table 9.2. [2] P. Papka et al., Phys. Rev. C **75**, 045803 (2007).

All fixed inputs reproduce the three Pochodzalla structures

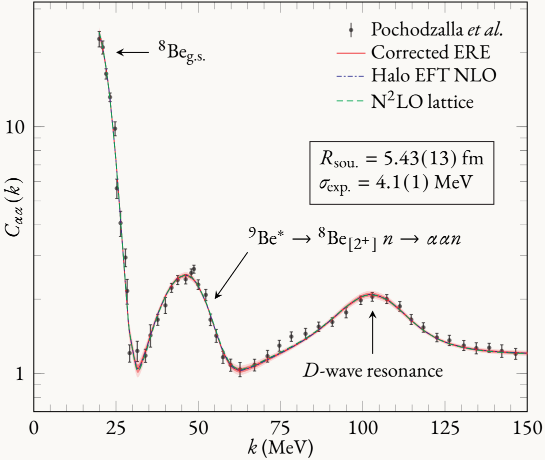

INFERRED STRUCTURES

0^+ pole broadened by resolution; ^{9}Be shoulder with endpoint at 56.5 MeV; broad 2^+ resonance near $p \sim 100$ MeV.

FITTED

$R \simeq 5.4$–5.6 fm,

$\sigma_p \simeq 4.1$–4.3 MeV.

RESULT / LIMIT

ERE and halo EFT nearly coincide; all fixed inputs give comparable fits.

10^6 bootstrap samples; point errors $\times 3.5$; constrained residual background marginalized.

Ghetti: R is input-stable; β remains sensitive

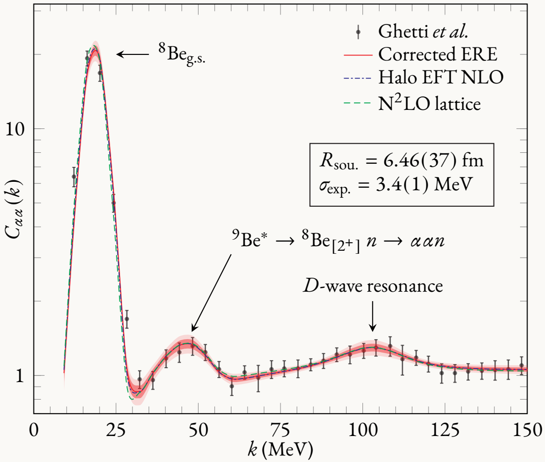

FITTED AT 44 MeV/NUCLEON

$R \simeq 6.4$–6.5 fm,

$\sigma_p \simeq 3.3$–3.4 MeV.

INFERRED

The same scattering inputs are used across data sets. The radius is stable across the three inputs; the lattice input mainly lowers the fitted β.

LIMIT

The residual background is compatible with zero. Present fit differences do not select a unique interaction.

R changes between data sets; β carries the input dependence

INFERRED: R separates the data sets; β separates the fixed scattering inputs.

FITTED PARAMETERS

Fit quantity	Pochodzalla	Ghetti (44 MeV/A)
R across inputs (fm)	5.43–5.58	6.42–6.47
σ_p across inputs (MeV)	4.09–4.25	3.29–3.40
β, corrected ERE	0.61 ± 0.03	0.40 ± 0.10
β, halo EFT NLO	0.60 ± 0.04	0.38 ± 0.10
β, N^{2}LO lattice	0.33 ± 0.05	-0.03 ± 0.17

RESULT

ERE and halo EFT give nearly equal β; lattice lowers it and is compatible with zero for Ghetti.

LIMIT

Conditional on source, resolution and composition; no unique interaction is selected.

Bootstrap separation is largest in β

INFERRED FROM 10^6 PSEUDOEXPERIMENTS: ERE and halo EFT remain nearly coincident; the lattice input shifts R and σ_p upward and β downward.

Momentum resolution

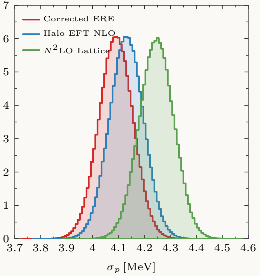

Source radius

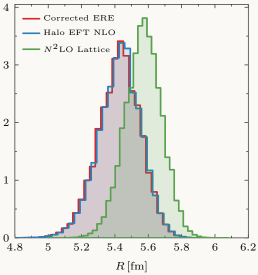

Finite-range coefficient

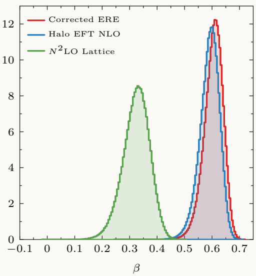

LIMIT: point errors are multiplied by 3.5; background nuisance parameters are marginalized. The panels show one-dimensional marginals only; joint correlations and the full theory-error budget are not shown.

Femtoscopy retains information beyond the on-shell amplitude

At fixed on-shell scattering input, the correlation retains a source-weighted interior contribution that must be matched to the exterior wave.

FORMALISM

Nonperturbative Coulomb and a Coulomb-modified effective-range amplitude.

An effective-range identity fixes the nominal S-wave interior norm.

Exterior and interior terms require a common short-distance prescription.

FIXED INPUTS, FITTED RESPONSE

pp: finite-range terms remove most of the exterior-wave excess; source variation limits the constant-source approximation.

$\alpha\alpha$: fixed $S + D$ inputs describe Pochodzalla and Ghetti after fitting source, feed-down and resolution.

INFERRED: weak input dependence of R; stronger sensitivity in β.

LIMIT AND OUTLOOK: current fits show finite-range sensitivity without selecting a unique interaction. More precise $\alpha\alpha$ data and controlled short-distance matching for $\ell > 0$ are required.

B1. Proton correlations with the Reid soft-core potential

Question: Does LL+FRP converge to the Reid/Koonin result as R grows?

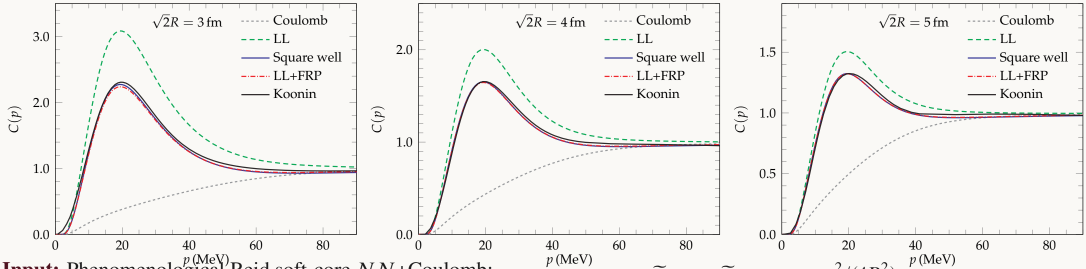

Input: Phenomenological Reid soft-core NN+Coulomb; Koonin uses numerical pp waves, while LL and LL+FRP share the $^1S_0$ ERE.

Equation: $\widetilde{S}_R(r)/\widetilde{S}_R(0) = e^{-r^2/(4R^2)} \to 1$ for $R \gg R_S$.

Evidence: LL remains high, while LL+FRP approaches Koonin across $\sqrt{2}R = 3, 4, 5$ fm. **Validity:** The convergence comes from reduced source variation, not from changing the amplitude.

R. V. Reid, Ann. Phys. **50**, 411 (1968); S. E. Koonin, Phys. Lett. B **70**, 43 (1977). Formalism paper, Fig. 2.

B2. Coulomb-modified norm identity and $d_0(p)$

Question: What interior norm does the Coulomb-subtracted ERE fix?

Input: Coulomb-subtracted ERE

$$K_0(p) = \mathrm{Re}\, f_{SC}^{-1}(p) + 2\lambda\alpha\mu h^{\lambda}(\eta), \\ = -\frac{1}{a_0} + \frac{1}{2} r_0 p^2 + v_2 p^4 + \cdots ,$$

$$d_0(p) = 2\frac{\partial K_0}{\partial p^2} = r_0 + 4v_2 p^2 + \cdots .$$

Equation: exterior–interior norm

$$\frac{d_0(p)}{2} C_\eta^2 |f_{SC}(p)|^2 = \int_0^\infty dr\, r^2 \\ \times \left(|\phi_0^{\mathrm{asy}}|^2 - |\phi_0^{\mathrm{exact}}|^2 \right).$$

Evidence: momentum dependence

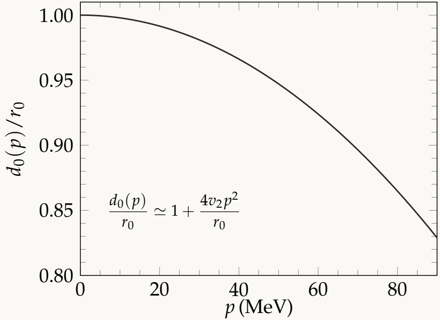

$d_0/r_0 : 1 \to 0.83$ by 90 MeV; v_2 sets the curvature.

Validity: Local, energy-independent, finite-range strong potential; both waves retain Coulomb, and $d_0(0) = r_0$. Formalism paper, Eq. (63), Fig. 3.

B3. Source weighting and the finite-range coefficient β

Question: Is β bounded between zero and one?

Input: $I(r,p) = r^2\left(|\phi_0^{\text{exact}}|^2 - |\phi_0^{\text{asy}}|^2\right)$.

Equation: $\delta C = 4\pi \int dr\, \widetilde{S} I \simeq 4\pi\beta\widetilde{S}(0) \int dr\, I$.

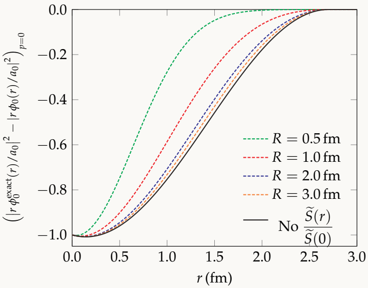

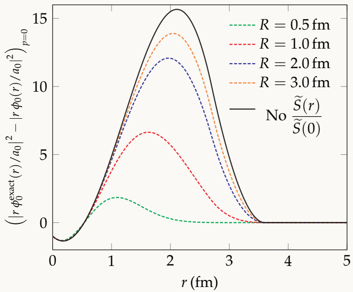

Evidence: no barrier — for a Gaussian source, sign-definite I gives $0 \leq \beta \leq 1$, if the ratio exists.

Evidence: barrier — cancellations allow $\beta \notin [0,1]$, with dependence on p, R, and the interaction.

Validity: Neutral np examples; Coulomb and identical-particle statistics omitted. β is a source-weighting coefficient, not a probability.

B4. ALICE pp: scattering input and residual correlations

Question: What is fixed in ALICE, and how is $p\Lambda$ feed-down mapped?

Input: fixed scattering, source, and composition

Input	Value
a_0	-7.78 fm
r_0	2.72 fm
v_2	$-0.028\, r_0^3$
R	$1.249(8)(24)$ fm
λ_{pp}	0.67
λ_{pp_Λ}	0.203
β	1

[1] S_0 Reid soft-core parameters; Gaussian source radius and pair fractions from ALICE.

Equation: observed correlation

$$C'(p) = 1 + \lambda_{pp}[C_{pp}(p) - 1] + \lambda_{pp_\Lambda}[C_{pp_\Lambda}(p) - 1].$$

Evidence: residual-correlation map

$C_{p\Lambda}$ input

$\downarrow$

$\Lambda \to p\pi^-$: decay kinematics

$\downarrow$

C_{pp_Λ} in the pp momentum basis

Remaining flat components stay in the unit baseline.

Validity: No parameter is refitted. Bands propagate only the Gaussian source-radius errors; other model uncertainties are excluded.

B5. $\alpha\alpha$ ERE inputs and near-threshold poles

Question: How stable is the 0^+ pole across fixed inputs?

Input: ERE convention

$$K_0(p) = -\frac{1}{a_0} + \frac{1}{2} r_0 p^2 - \frac{P_0}{4} p^4 + \cdots, \qquad P_0 = -4v_2.$$

Equation: pole condition

$$f_0^{-1}(p_\star) = 0, \qquad \frac{p_\star^2}{2\mu} = E_R - \frac{i\Gamma_R}{2}.$$

Evidence: pole positions implied by each input

Input	a_0 10^3 fm	r_0 fm	P_0 fm^3	E_{0^+} keV	Γ_{0^+} eV
Corrected ERE	−1.92(9)	1.099(5)	−1.62(8)	92.3(5.5)	5.7(4.0)
Halo EFT NLO	−1.92(9)	1.098(5)	−1.46(8)	91.1(5.4)	4.9(3.5)
$\mathrm{N^2LO}$ lattice	−1.55(63)	1.061(14)	−2.277(158)	88.2	2.98

Validity: 10^6 independent Gaussian ERE samples, with no covariance matrix. Lattice central values are shown; its non-Gaussian ensemble also contains virtual-state solutions. Manuscript Tables I–II; inputs are fixed before the CF fits.

B6. $\alpha\alpha$ fits: bootstrap and nuisance parameters

Question: What do the two bootstrap error budgets include?

Input: 10^6 bootstrap pseudoexperiments per data set.

Evidence: data-set-specific treatment

Treatment	Pochodzalla	Ghetti, 44 MeV/nucleon
Point errors	Multiplied by 3.5 before bootstrapping	Published point errors
Background	Gaussian-prior nuisance parameters; marginalized	Compatible with zero; omitted
Radius selection	—	Samples with $R > 7.9$ fm excluded

Equation: Pochodzalla residual background

$$B_d(p) = \frac{M_{\rm bg}}{2}\left[-1 + \tanh\left(\frac{p - p_{\rm bg}}{\Delta_{\rm bg}}\right)\right], \qquad \Delta_{\rm bg} = 2\,\mathrm{MeV}.$$

Validity: Bootstrap standard deviations are conditional on the Gaussian source, kernel, resolution, cuts, and fixed scattering input. Reduced χ^2 values are not directly comparable across the two error prescriptions.

B7. Short-distance matching for higher partial waves

Question: Why does the D wave require its own short-distance matching?

Input: regular physical interior

$$\Psi_\ell^{\text{exact}}(r,p) = O(r^\ell),$$

$$r^2 S_R(r)|\Psi_\ell^{\text{exact}}|^2 = O(r^{2\ell+2}).$$

The source integral converges at $r = 0$.

Evidence: singular exterior continuation

$$\mathcal{G}_{C;\ell}^{(+)}(r,p) \sim r^{-\ell-1},$$

$$r^2 S_R(r)|\Psi_\ell^{\text{ext}}|^2 \sim r^{-2\ell}.$$

For $\ell = 2$, the leading radial integrand is r^{-4}.

Equation: matched physical contribution

$$\Delta C_\ell^{\text{phys}} = \lim_{\epsilon\to 0}[\Delta C_\ell^{\text{ext}}(\epsilon) + \Delta C_\ell^{\text{match}}(\epsilon)].$$

Established S-wave result

$$\Delta C_{\text{FRP},0}^{(E)} \simeq -4\pi d_0(p) C_\eta^2 |f_0(p)|^2 S_R(0).$$

Validity: D-wave completion

The exterior and matching terms require one common short-distance prescription, followed by a stability study of their sum.

The explicit norm identity is established for $\ell = 0$; higher waves require separate matching. Manuscript discussion after Eqs. (10), (12), and (13).

B8. References and experimental inputs

Question: Which reference fixes each analysis layer?

Equation: Coulomb and finite-range formalism

M. Albaladejo, A. García-Lorenzo and J. Nieves,
Femtoscopy Correlation Functions and Hadron–Hadron Scattering Amplitudes in Presence of Coulomb Potential.
PTEP **2025**, 093D02; DOI: 10.1093/ptep/ptaf095.

Input: elastic scattering

R. Higa, H.-W. Hammer and U. van Kolck, Nucl. Phys. A **809** (2008) 171–188.
Halo EFT and corrected $\alpha\alpha$ ERE.
S. Elhatisari *et al.*, JHEP **02** (2022) 001.
Nuclear-lattice $\alpha\alpha$ input.

Application: current status

A. G. Lorenzo, M. Albaladejo, A. Feijoo and J. Nieves,
Femtoscopy as a new venue for nuclear physics: $\alpha\alpha$ scattering.
Manuscript in preparation.

Evidence: benchmarks and data

S. E. Koonin, Phys. Lett. B **70** (1977) 43–47.
ALICE, Phys. Lett. B **805** (2020) 135419.
J. Pochodzalla *et al.*, Phys. Lett. B **161** (1985) 275–279.
R. Ghetti *et al.*, Phys. Rev. C **70** (2004) 027601.

Validity: The PTEP formalism is published; the $\alpha\alpha$ analysis remains a manuscript in preparation. Each citation supports a distinct analysis layer.